

G-  
IN-93-CR

5406

P 24

**FINAL REPORT**  
on  
**Bevalac Studies of Magnet Cerenkov Spectroscopy**  
**(NASA Grant NAG5-878)**  
**5 April 1991**

**1. Introduction**

NASA grant NAG5-878 was intended to support experimental tests of the magnet/Cerenkov method of resolving cosmic ray isotopes, such as have been proposed for use with Astromag, the superconducting magnet facility for particle astrophysics. In particular, we have been attempting to identify the various contributions to the velocity resolution of Cerenkov detectors such as might be used in Astromag, to measure the magnitude of these contributions and assess their effect on the mass resolution of an isotope spectrometer for Astromag, and to perform Bevalac tests of magnet/Cerenkov spectrometry. In addition, we have purchased and tested a first version of a new 5-inch photomultiplier tube that is designed for use in large magnetic fields. In this final report we summarize the results of the various activities funded under this grant over the period from 15 August 1987 to 14 October 1990.

At the time when this grant was first funded the NASA Astromag Definition Team was nearing completion of a pre-phase A study of the Astromag facility for Space Station Freedom (SSF). The Astromag facility, along with three first-generation experiments, was subsequently selected for flight on SSF in 1989. However, in late 1990, NASA announced an indefinite postponement of all attached payloads, including Astromag. Recently a study by Goddard Space Flight Center has shown that Astromag could be successfully flown as a free flyer (FF). The results of the work reported here have application to both the SSF and FF versions of Astromag.

**2. Approach**

The magnet/Cerenkov method for resolving isotopes is described in detail in Mewaldt (1986) and is also summarized in the Astromag Report (Ormes et al. 1986). Briefly, we describe the Cerenkov signal (in units of photoelectrons) as:  $L = L_0 Z^2 (1 - p_0^2/p^2)$  where  $L_0$  is the number of photoelectrons resulting from  $\beta=1$ ,  $Z=1$  nuclei and where  $p_0$  is the Cerenkov threshold in momentum/amu. The measured deflection ( $X$ ) due to the magnetic field can be expressed as  $X = (kZ/pA)$ , where  $k$  (which is approximately proportional to  $\int B \times dl$  and depends on the trajectory) can be treated as a constant for our purposes. Solving for the mass  $A$  (in amu):

$$A = \left( \frac{kZ}{Xp_0} \right) \left( 1 - \frac{L}{Z^2 L_0} \right)^{\frac{1}{2}}$$

Contributions to the mass resolution of such a spectrometer can be

analytically evaluated by taking appropriate partial derivatives of the above expression (see, e.g., Mewaldt 1986).

### 3. Bevalac Studies of Cerenkov Radiators

A major goal of this work was to obtain Bevalac exposures of aerogel Cerenkov radiators at the Lawrence Berkeley Laboratory Bevalac in order to learn more about their response and resolution. In the fall of 1987 we completed construction of a Cerenkov light-integration box employing four 5" Amperex photomultipliers and conducted calibrations of the box using light-emitting diodes (LEDs) and cosmic ray muons. The inner dimensions of the box were approximately 25 cm x 25 cm x 20 cm, and it was designed to permit rapid change out of a variety of radiators with typical dimensions 14 cm x 14 cm or less. This Cerenkov test box was taken to the Bevalac in November of 1987 and used in calibrations of a variety of Cerenkov radiators, including several samples of aerogel with indices of refraction ranging from 1.08 to 1.15, provided by Ib Rasmussen of the Danish Space Research Institute. The aerogel calibrations were carried out using a 1700 MeV/nucleon  $^{56}\text{Fe}$  beam, well above the aerogel threshold, while calibrations of other radiators were done with beams ranging from N to Fe.

Included in the experimental setup was a multiwire proportional counter that could measure the position of individual particles to an accuracy of  $\sim 1$  mm, and two scintillators, 10 cm x 10 cm in area, that were centered on the radiators and used to provide a coincidence trigger pulse. A calibrated system of copper absorbers upstream of the LBL Beam-40 spectrometer magnet could be used to degrade the beam energy.

### 4. Bevalac Data Analysis and Results

Analysis of the Bevalac data has provided information on a variety of properties of aerogel Cerenkov radiators and their use to provide velocity resolution in the GeV/nucleon energy region, including:

- Measurement of the degree of self-absorption of Cerenkov light when two aerogel blocks are stacked back-to-back.
- Measurement of the energy (velocity) dependence of the light yield for comparison with theoretical models of Cerenkov light production.
- Investigation of variations of the index of refraction within a block of aerogel.
- Measurement and comparison of the yield of Cerenkov light from several aerogel samples of varying index of refraction.

Examples of these results are summarized briefly below.

#### 4.1 Dependence of Yield on Aerogel Thickness

Analysis of Bevalac data has shown that there is about a 20% decrease in the light output (per block) when two aerogel blocks are stacked back-to-back. We have now derived a formula that accounts for this self-absorption in terms of an effective absorption mean free path and find  $\lambda_a \simeq 4$  cm for index  $n=1.1$ . This is somewhat smaller than published values of  $\lambda_a$  for other indices, but it is probably consistent when we take into account the fact that the Cerenkov light is emitted at an angle of  $\theta \simeq 65$  deg. This implies that there is a point of diminishing returns if one attempts to increase the light output of such an aerogel radiator by making it thicker.

#### 4.2 Agreement with the Cerenkov Relation

If the measured yield of Cerenkov light is plotted against the quantity  $1/\beta^2$ , one expects a linear relationship. This is demonstrated in Figure 1. The intercept of this linear yield with the approximately flat background of light due to radiation from the paint and to knock-on electrons can be used to determine the index of refraction (see below).

#### 4.3 Index of Refraction Variations

One of the concerns in optimizing the resolution of aerogel Cerenkov radiators has been the effect of possible variations in the index of refraction over the area of the blocks. Such variations can masquerade as light collection variations, but would have a different effect on the derived mass of an incident nucleus. In order to separately identify these two effects it is possible to calibrate or "map" the radiator at two or more separate energies. In analyzing an aerogel radiator with an index of refraction of 1.12, we found that the index was indeed not constant. Figure 1 shows the light yield from two separate  $2 \times 2$  cm<sup>2</sup> spots of a block of aerogel radiator, plotted versus  $1/\beta^2$ . From the intersection of a fit to this response the index of refraction can be determined, as well as the yield of Cerenkov light. In this case it is found that the index varies from 1.1209 to 1.1225 between these two locations, while the actual light collection was the same to within 0.3%. This degree of nonuniformity was not typical; most blocks were found to be considerably more constant in index.

The index of refraction variation in Figure 1 would amount to an unacceptably large deviation in the mass resolution if it were not "mapped" and corrected for. From an analytical calculation it has been determined that the effect of such a variation on the mass resolution would be:

$$\Delta M = \frac{Mn}{(n^2-1)} \Delta n$$

where M is the mass in amu. For <sup>56</sup>Fe this amounts to  $\Delta M = 0.4$  amu, which is, of course, significant. Fortunately, calibrations such as these illustrate an effective way of mapping such variations.

In an effort to understand the scale and magnitude of the index variation a least-squares fit was done to the observed resolution of the signal (at several beam energies), taking into account photoelectron statistical variations, light collection variations, and index of refraction variations. Figure 2 is a contour plot of the chi-squared of that fit as a function of the number of photoelectrons/ $Z^2$  and the residual index variation  $\sigma_n$ . From independent calibrations with cosmic ray muons we can fix  $N_\mu$  at  $12 \pm 2$  photoelectrons, which implies  $\sigma_n \simeq 0.0008$ . It is encouraging that the Bevalac photoelectron result for Fe agrees with the muon result, which has not always been true in some earlier studies of other radiators.

## 5. Contribution to Cerenkov Resolution from Knock-on Electrons:

One of the contributions to the Cerenkov resolution that we have investigated under this grant is the effect of Cerenkov light produced by knock-on (KO) electrons that have velocities above the Cerenkov threshold ( $\beta > n^{-1}$ ).

Such knock-ons (also called  $\delta$ -rays) can be created in the radiator itself, and in overlying material, and the light that they produce is added to the "primary" Cerenkov light from the particle itself. Statistical fluctuations in the number and energy of knock-on electrons produced contribute to the uncertainty in the velocity measurements that are obtained from Cerenkov counters.

Figure 3 shows the expected contributions of "primary" Cerenkov light and " $\delta$ -ray" light as a function of energy for a radiator with  $n = 1.04$ . Note that a contribution of  $\delta$ -ray light is expected even when the primary particle is below the Cerenkov threshold because the maximum energy knock-on can have up to  $\sim 2$  times the velocity of the primary particle. Two separate approaches have been investigated to estimate the  $\delta$ -ray contribution and the fluctuations in this contribution.

### 5.1 Analytical Approaches

While a graduate student at Caltech, J.E. Grove developed a method for calculating the mean and standard error of the added Cerenkov contribution due to KO electrons. This work is reported in a paper contributed to the 21st International Cosmic Ray Conference (Grove and Mewaldt 1990), and it is now in the final stages of preparation for publication Nuclear Instruments and Methods (Grove and Mewaldt 1991). Figure 4 shows the mean and standard error of the added knock-on component for four different indices of refraction, and for various amounts of overlying material. When standard error estimated from this approach is applied to aerogel counters of an index such as that planned for Astromag ( $n \simeq 1.03$ ) we find that this contribution to the mass resolution is significant, but not dominant.

### 5.2 Monte Carlo Approaches

When the number of knock-ons that is created is small, so that "Gaussian" statistics do not rigorously apply, a Monte Carlo approach may be called for. Such an approach is all useful for investigating the "tails" of the

Cerenkov light distributions. Figure 5 shows a Monte-Carlo calculation of the expected yield from Fe nuclei in an aerogel radiator with  $n = 1.03$ , including the knock-on contribution that is evident below the Cerenkov threshold.

### 5.3 Cerenkov Light from Knock-ons in a High Magnetic Field

Although high energy knock-on electrons created in a thin radiator are likely to escape out the bottom of the radiator before slowing down thus making only a limited contribution to the total Cerenkov radiation, this is not necessarily the case in a high magnetic field. In the limit where  $B = \infty$ , the electrons simply spin around the local field and lose all their energy (and light) at the point they are created. In this situation we can anticipate somewhat greater contributions from knock-on electrons, and also somewhat larger fluctuations in the yield. Grove and Mewaldt (1991), found that in their approach the mean light yield and the standard error for  $B = \infty$  were identical to the case where there is an infinite overburden - in other words the knock-on electron population is in equilibrium.

In a more realistic situation where the magnetic field is not infinite, we can expect that the yield will depend on how the radius of curvature of the electrons compares with the thickness of the radiator and the proximity of any surrounding material where energy loss may take place.

As a quantitative example we consider a radiator of index  $n$  in a magnetic field of 1 kiloGauss (kG). The minimum energy knock-on that can produce Cerenkov radiation is  $E_{\min} = (\gamma_n - 1) m_e c^2$  MeV where  $m_e c^2 = 0.511$  MeV and  $\gamma_n = [n^2/(n^2 - 1)]^{1/2}$ . For nuclei at Cerenkov threshold the maximum energy knock-on that can be produced is given by  $E_{\max} = 2m_e c^2 (\gamma_n^2 - 1)$ . The radius of curvature  $r$  of these electrons in a field of  $B$  kilogauss is given by  $r(\text{cm}) \simeq 3.3P(\text{MV})/B(\text{kG})$ , where  $P$  is the rigidity of the electron in MV. Taking  $n = 1.05$  and  $B = 1$  kG we find  $E_{\min} = 1.2$  MeV,  $E_{\max} = 10$  MeV, with corresponding values of  $r_{\min} = 5$  cm and  $r_{\max} = 35$  cm. These values are indeed comparable to the thickness and dimensions of typical Cerenkov radiators, suggesting that a Monte Carlo approach may be required to evaluate this contribution if an accurate estimate is required.

For the aerogel Cerenkov counters in the SSF design for Astromag we have  $B \simeq 0.6$  kG and  $n = 1.03$  or  $n = 1.04$ , in which case the radii of curvature of interest range from  $\sim 10$  cm to  $\sim 100$  cm. Monte Carlo calculations were performed assuming that for  $r \leq 10$  cm the electrons lose all their energy in the radiator, for  $r \geq 35$  cm they lose none of their energy in the radiator (once they have escaped); for  $10 \leq r \leq 35$  cm it was assumed that the fraction of energy lost in the radiator (once they had escaped the first time) was given by  $f = (35 - r)/25$ . Note that the height of the LISA Cerenkov boxes is  $\sim 17$  cm. Figure 6 shows the results of a Monte Carlo simulation of the resulting mass resolution. With these approximations it was found that the values of the mean and standard error were reasonably well approximated by the  $B = \infty$  case, indicating that this contribution should not be a major problem in the SSF design for LISA.

## 6. A Large-Area Photomultiplier for Use in High Magnetic Fields

In October of 1988 we applied for and were granted a supplement to this proposal for the purpose of purchasing and testing the first model of a new 5"-diameter photomultiplier tube (PMT) under development by the Hamamatsu Corporation. This tube is especially designed for use in high magnetic-field applications (up to 10 kG) such as Astromag, and it should be particularly useful in Cerenkov counters for that facility. The new 5" PMT is similar in design to a 2" PMT developed earlier by Hamamatsu (Model 2490), but more than nine times larger in active photocathode area. A study that we conducted prior to Hamamatsu's decision to manufacture this tube showed that in typical applications a 5"-design offered >75% better efficiency in light collecting power when compared to the 2" design. In addition, the the larger area tube will also lead to weight and power savings in space applications.

The first version of this tube (Model R4084) was delivered in the fall of 1989 (see Figure 7). Following laboratory tests it was taken to the Bevalac in April of 1990 where a uniform magnetic field ranging from 0.5 to 3 kG was made available through arrangements with H. C. Crawford. A special mounting fixture was fabricated to vary the alignment of the tube with respect to the field direction and two LEDs were used to provide a source of light.

Figures 8 through 11 summarized the results of these magnetic field tests. Figure 8 shows the relative gain of the PMT as a function of the angle  $\theta$  with respect to the field direction. The unexpected result that the gain at 0.5 kG increases for  $\theta > 0$  apparently indicates magnetic focusing effects within the tube. In Figure 9 these same data are plotted as a function of field strength (normalized to  $B=0$ ,  $\theta=0$ ), while Figure 10 shows the dependence of the relative response in PMT high voltage for two field strengths. Finally, in Figure 11 we show the relative number of photoelectrons (PEs) as determined from the width of the distributions, as a function of angle and field strength. The fact that the PE yield in Figure 11 does not scale exactly with the gain (Figure 8), indicates that some of the effects of the field are occurring beyond the first stage, probably because of magnetic focusing effects.

Overall, the performance of this first version of the R4084 5" tube are very encouraging. It is clear from Figures 8 and 11 that the tube can operate in fields up to 3 kG at a level that compares favorably with its performance at  $B = 0$ . Although some of the dependence on field direction and magnitude is not yet understood, these data have been provided to Hamamatsu for use in designing an improved version of this tube.

Measurements of the photoelectron yield of the R4084 tube and of standard Amperex 5" PMTs were made using on LED by graduate student Alan Laborador. It was found that the first version of the R4084 gave 55% of the photoelectron yield of the Amperex tubes. This is one area that Hamamatsu hopes to improve in subsequent versions of this tube.

**7. Aerogel Transmission Tests** During the summer of 1988 we conducted some new tests of aerogel light transmission properties in an effort to help understand the Cerenkov light yield from these radiators. Using a spectral

photometer in the Geology Department at Caltech we measured the light transmission of several aerogel samples of various index of refraction. Figure 12 includes examples of such data for several indices of refraction. Note that the "transmission" declines rapidly at shorter wavelengths. This decline is actually a combination of the scattering and absorption mean free paths, since in the setup used, light that is scattered out of the beam is no longer measured, even though it might be recovered in a counter of the "integrating" design typically used for Cerenkov counters. However, the significant decline does point to the importance of developing means to collect a greater fraction of the short wavelength light, perhaps by wave-shifting techniques, since this is the region where the bulk of Cerenkov light emission is concentrated.

This technique has been used to test the effect that machining the block's surface (for uniformity purposes) has on the light transmission, since there is an indication that machined blocks have a lower light output than unmachined blocks (see e.g., Figure 12).

One concern in using aerogel radiators is their stability. We have previously observed a decrease in the light output of a few % per month from blocks that were continuously installed in a counter over a period of several years. We now suspect high-reflectance  $\text{BaSO}_4$  paint (on the walls of the box) as the cause of this degradation. We are currently storing our aerogel blocks in a dry air atmosphere. Tests over the past year have shown no change  $>7\%$ , so this seems to be a reasonably safe environment. We are now planning to investigate whether the use of Millipore filter paper as a high-reflectance coating for the counter walls will give an acceptable light output, since it is known that this paper is compatible with aerogel over several year time scales. Transmission measurements such as those shown in Figure 12 are also useful for monitoring aerogel contamination by other materials.

## **8. Magnet/Cerenkov Spectroscopy**

### **8.1 Mass Resolution Assessments**

A first analytical assessment of the contributions to the mass resolution of a magnet/Cerenkov isotope spectrometer was reported in Mewaldt (1986). It included the effects of photoelectron statistics, finite rigidity resolution in the spectrometer, and mapping uncertainties. In the course of the work under this grant we have considered two additional contributions, delta-ray fluctuations, and index of refraction variations, and we have made some preliminary assessments and measurements of the magnitude of these effects in aerogel radiators. (below the aerogel Cerenkov threshold from Cerenkov radiation in the paint.) Figure 13 shows an example of mass resolution calculations that include the above effects as well as others, for a counter such as that being considered for use in Astromag. Note this counter would provide mass resolution from  $\sim 2.1$  to 3 GeV/nucleon; this energy range could be extended by use of additional counters of either similar or lower index of refraction.

## 8.2 Mass Resolution Testing

When this work was begun it was hoped that an experimental simulation of the magnet-Cerenkov spectroscopy approach might be possible using a combination of a) the Beam-40 bending magnet at the LBL Bevalac; b) a multiwire proportional counter to measure position; and c) a Cerenkov counter. In the Beam-40 spectrometer the bending magnet can be used to deflect the beam over a distance ( $X$ ) of anywhere from 10 to 200 cm, so that the isotopes of a given element should in principle be separated by  $\Delta X \simeq \Delta A/A$  cm. This separation could in principle be measured by the proportional counter if we select, for example, particles that all have the same velocity from a beam of fragmentation products.

Conversations with Bevalac personnel convinced us that the Beam-40 situation was much more complicated than anticipated (H.C. Crawford, private communication), and so this approach was abandoned. Apparently, in the Beam-40 spectrometer there is a certain amount of focusing that also takes place for deflected particles, with the result that beams of different rigidities do not all focus at the same "depth" from the magnet. Thus it did not appear possible to focus multiple isotopes of an element at the same time and location. As a result, Bevalac personnel convinced us that our limited beam time was better spent pursuing other investigations.

## 8.3 The Venice Conference on Physics and Astrophysics in the Space Station Era

In January of 1988 a paper (Mewaldt and Ormes, 1989) discussing the measurement of cosmic ray isotopes with Astromag was presented at the Venice Conference on Physics and Astrophysics in the Space Station Era, held in October of 1987. Included in this paper was a discussion of the experimental approach to measuring cosmic ray isotopes that is under study here. Although plans for R. A. Mewaldt to attend this conference unfortunately had to be canceled, the paper was presented at the conference by J. O. Ormes. A written version of the paper is published in the proceedings of the conference (Mewaldt and Ormes 1988).

## 9. Summary

The work funded under this grant has identified, and allowed better estimates of, several contributions to the mass resolution of a cosmic ray isotope spectrometer such as might be used with Astromag. These include index of refraction variations and knock-on electron production of Cerenkov light. In addition, a new 5-inch PMT, such as will be required by Astromag, has been successfully tested. This work provides a much firmer basis for concluding that Astromag can accomplish its scientific objectives in cosmic ray isotope spectroscopy.

**Acknowledgments:** We appreciate the significant contributions of J.E. Grove to several aspects of this work during the period while he was a graduate student at Caltech. Grove performed the data analysis shown in Figure 2 and was responsible for calculations of the Cerenkov contribution due to knock-on electrons. Important contributions to this work were also made by graduate students Tim Shippert, who performed the Monte Carlo calculations in Figures 5 and 6, and Allan Laborador, who evaluated the photoelectron yield of the R4084 PMT. We are also grateful to S.M. Schindler for performing the magnetic field tests. Finally, the assistance of Hank Crawford of Lawrence Berkeley Laboratory is gratefully acknowledged.

### References

Of the references below, those marked with a star (\*) were funded in part by this grant.

\*J. E. Grove and R. A. Mewaldt, "Contribution to Cerenkov Resolution from Knock-on Electrons", Proceedings of the 21st International Cosmic Ray Conference, Adelaide, 4, 398 1990.

\*J. E. Grove and R. A. Mewaldt, "Contribution to Cerenkov Resolution from Knock-on Electrons", to be submitted to Nuclear Instruments and Methods, 1991.

R. A. Mewaldt, "Measurements of Cosmic Ray Isotopes with a Super-Conducting Magnet Facility", in the Proceedings of the Workshop for Scientific Uses of the Space Station, J. Klarmann, editor, p. 140, 1986.

\*R. A. Mewaldt and J. F. Ormes, "Galactic Cosmic Ray Spectroscopy from the Space Station", in Physics and Astrophysics in the Space Station Era, P. L. Bernacca and R. Ruffini, editors, Bologna, 1989.

J. F. Ormes, M. Israel, M. Wiedenbeck, and R. A. Mewaldt, editors, "Astromag - The Particle Astrophysics Magnet Facility", Interim Report of the Astromag Definition Team, August 1986.

### Figure Captions

Figure 1: A plot of the measured relative light yield vs.  $1/\beta^2$  for two different positions of an aerogel radiator with nominal index  $n=1.12$ . Note that the index of refraction depends on position.

Figure 2: Chi-squared contour plot of the number of photoelectrons (divided by  $Z^2$ ) vs. the rms index of refraction variation, for an aerogel block with index 1.12. The plot was computed by graduate student Eric Grove from a fit to the measured light output at 5 different  $^{56}\text{Fe}$  beam energies. An independent calibration from muons gives  $12 \pm 2$  photoelectrons per  $Z^2$ , consistent with the Bevalac results.

Figure 3: Comparison of the "primary" Cerenkov light with that due to  $\delta$ -rays in a Cerenkov counter with  $n = 1.12$ . The number of  $\delta$ -rays produced depends on the thickness of the radiator (in this case 1.8 cm) and on the amount of overlying material, in this case taken to be  $0.25 \text{ g/cm}^2$ .

Figure 4: Calculations of the mean ( $K$ ) and standard error ( $\sigma$ ) of the Cerenkov light for four different indices of refraction (from Grove and Mewaldt 1990). The amount of overlying material is indicated.

Figure 5: Monte-Carlo calculation of the response of a Cerenkov radiator with  $n=1.03$  to Fe nuclei as a function of kinetic energy per nucleon. The light production below the nominal Cerenkov threshold of  $\sim 2.9 \text{ GeV/nucleon}$  (and some of the fluctuations in yield at higher energies) are due to knock-on electrons.

Figure 6: Monte-Carlo simulation of the mass resolution for Fe isotopes of a cosmic ray isotope spectrometer for Astromag that has Cerenkov radiators with  $n=1.04$  and  $n=1.03$ . The effect of the local magnetic field on knock-on electrons has been taken into account. Top panel: mass vs energy/nuc. Bottom panel: mass histogram of 2.5-3.5 GeV/nuc Fe isotopes. Note that the mass scale has not yet been correctly normalized.

Figure 7: Schematic of the new 5" tube being developed by Hamamatsu that was tested under this grant. The tube is designed to operate in magnetic fields of many kiloGauss.

Figure 8: Normalized response (relative to  $B=0, \theta=0$ ) of the R4084 PMT as a function of the angle ( $\theta$ ) of the tube with respect to the magnetic field direction, for different magnetic field strengths ( $B$ ) ranging from 0.5 kG to 3 kG.

Figure 9: Normalized response (relative to  $B=0, \theta=0$ ) of the R4084 PMT as a function of field strength ( $B$ ) for different angles ( $\theta$ ) with respect to the magnetic field direction.

Figure 10: Normalized response of the R4084 PMT as a function of the applied high voltage for two field strengths.

Figure 11: Relative photoelectron yield (normalized to  $B=0$ ,  $\theta=0$ ) of the R4084 PMT as a function of the angle ( $\theta$ ) of the tube with respect to the magnetic field direction, for different magnetic field strengths ( $B$ ) ranging from 0.5 kG to 3 kG.

Figure 12: An example of spectrophotometer measurements of the transmission as a function of wavelength of three different aerogel radiators. The sharp drop in transmission below 400 to 500 nm is due to Rayleigh scattering; much of this light can be recovered with a light integration box. For  $n=1.10$  data are shown both before and after a small section of the surface was machined, indicated the increased scattering and absorption that occur due to machining. Some, but not all of these machining losses can be recovered through polishing.

Figure 13: Calculated mass resolution for a magnet/Cerenkov spectrometer with Cerenkov counter having  $n = 1.03$  and  $1.04$ . Various contributions to the mass resolution are indicated, including photoelectron statistics (pe), knock-on electrons (ko), rigidity resolution (R, using  $MDR = 3.2$  TV), uniformity of light collection (u, assumed mapped to 0.003), multiple scattering (ms), and index of refraction variations (n, assumed to be mapped such that  $\sigma_n/(n-1) \simeq 0.0018$ ).

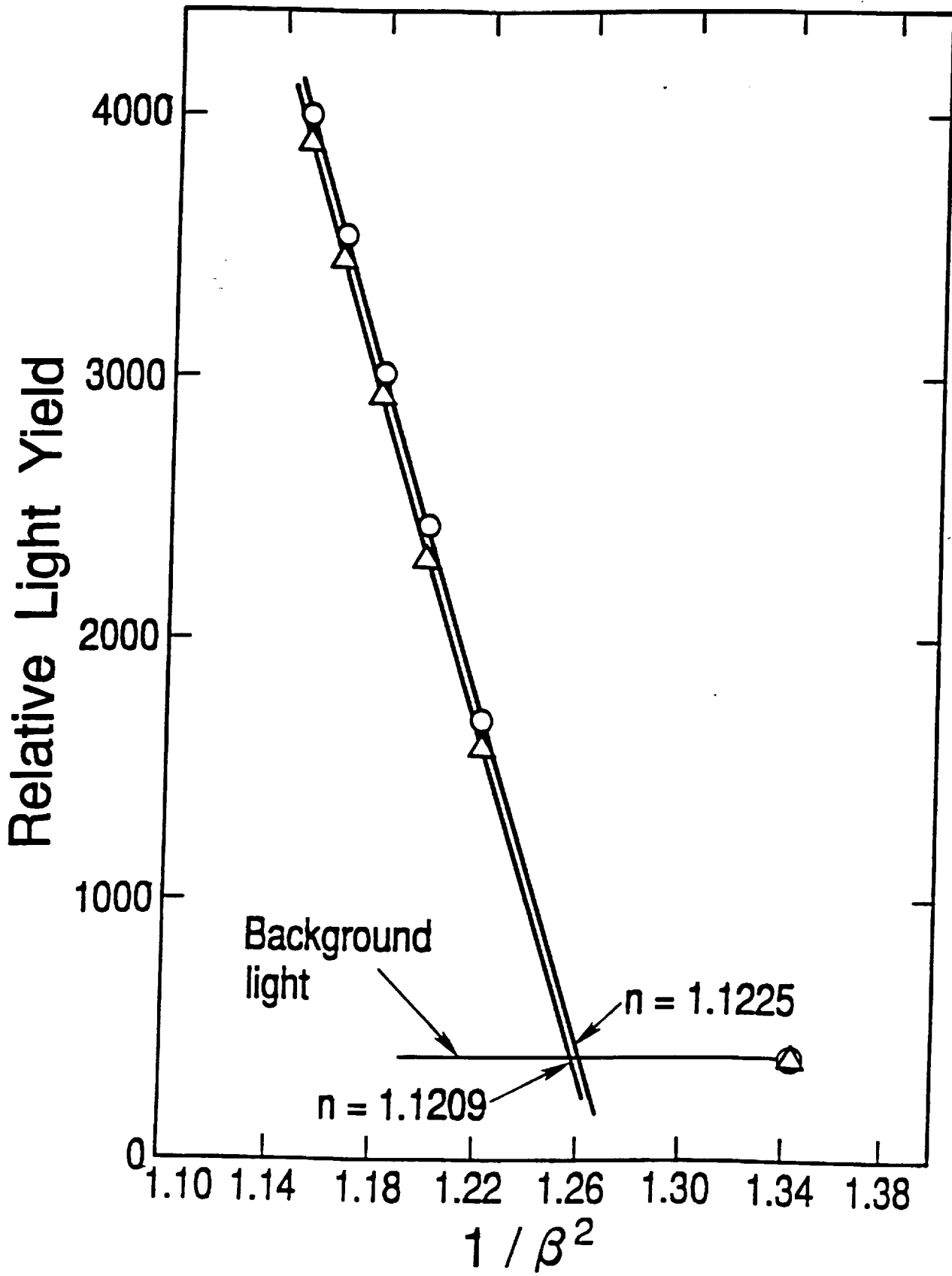
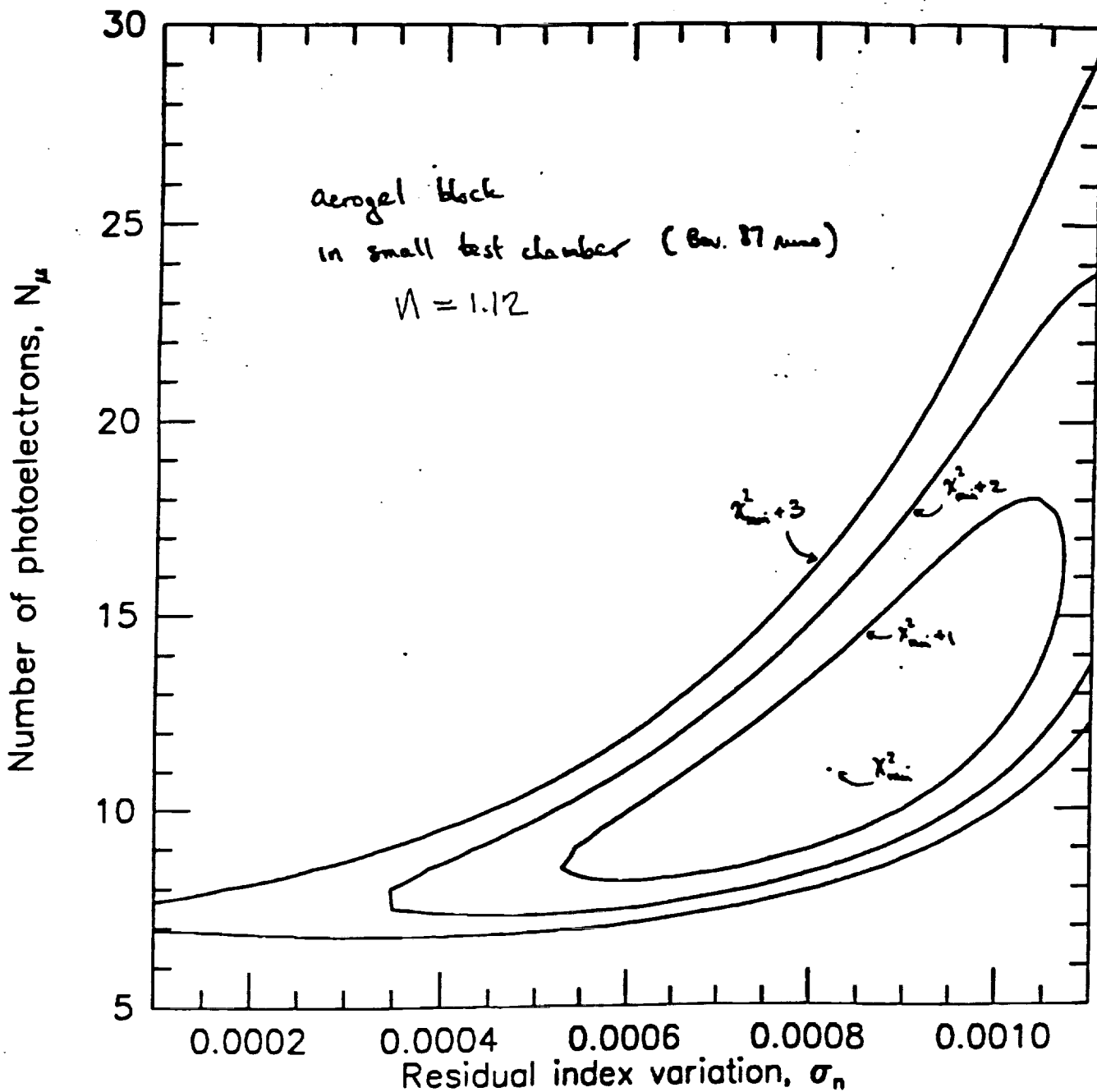


Figure 1



Chi-squared contour plot of the number of photoelectrons (divided by  $Z^2$ ) vs. the rms index of refraction variation, for an aerogel block with index 1.12. The plot was computed by graduate student Eric Grove from a fit to the measured light output at 5 different  $^{58}\text{Fe}$  beam energies. An independent calibration from muons gives  $12 \pm 2$  photoelectrons per  $Z^2$ , consistent with the Bevalac results.

Figure 2

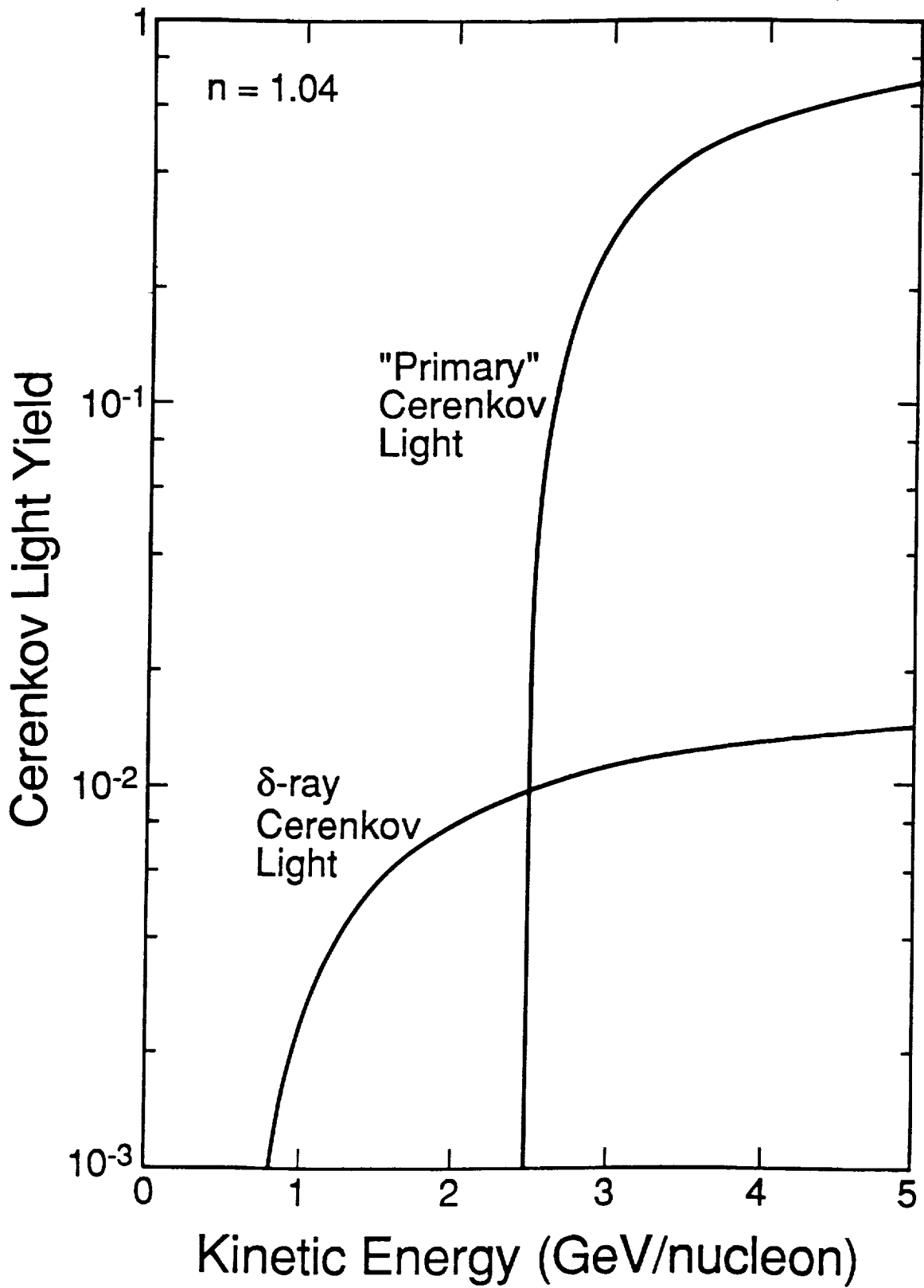


Figure 3

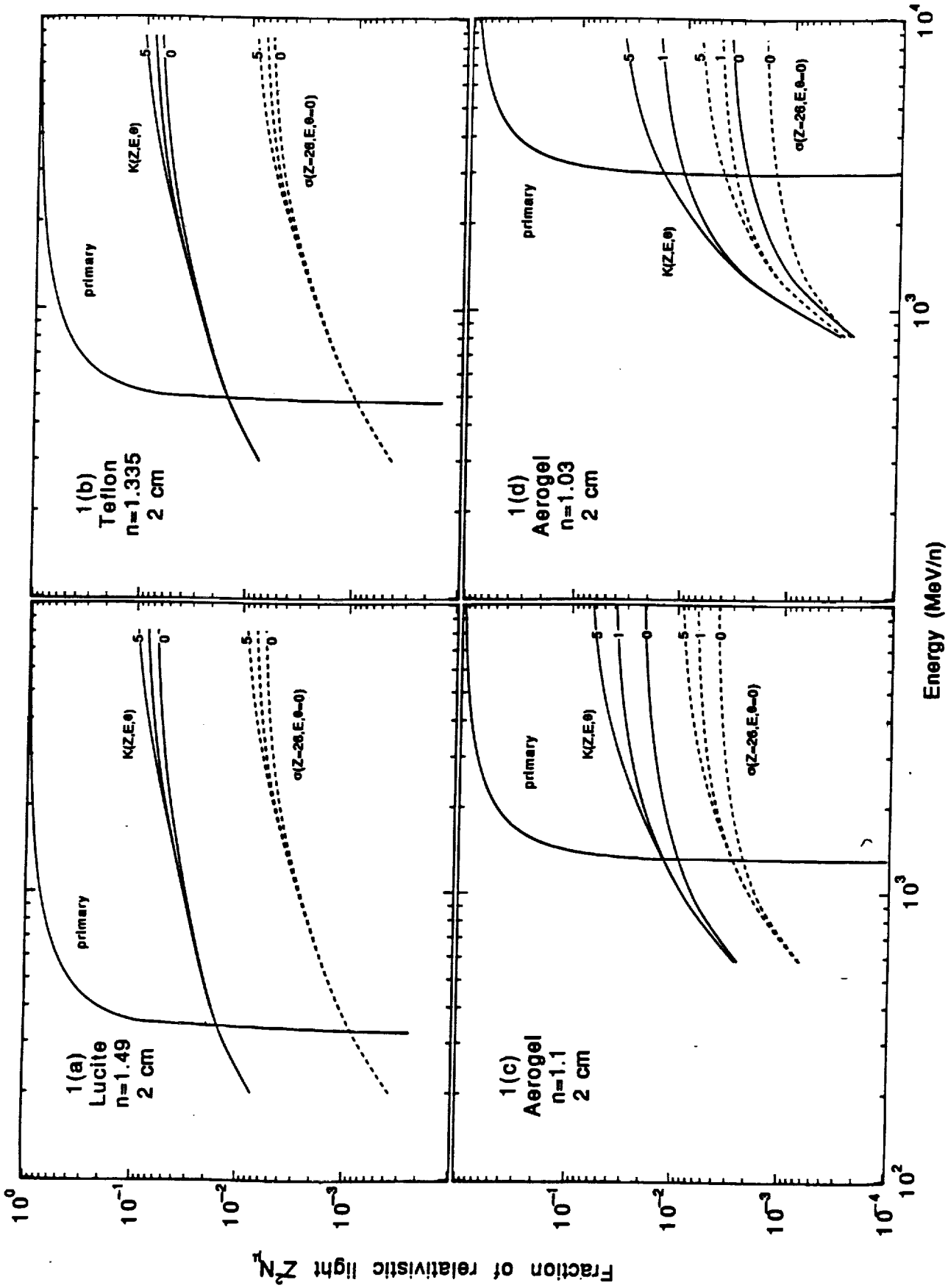


Figure 4

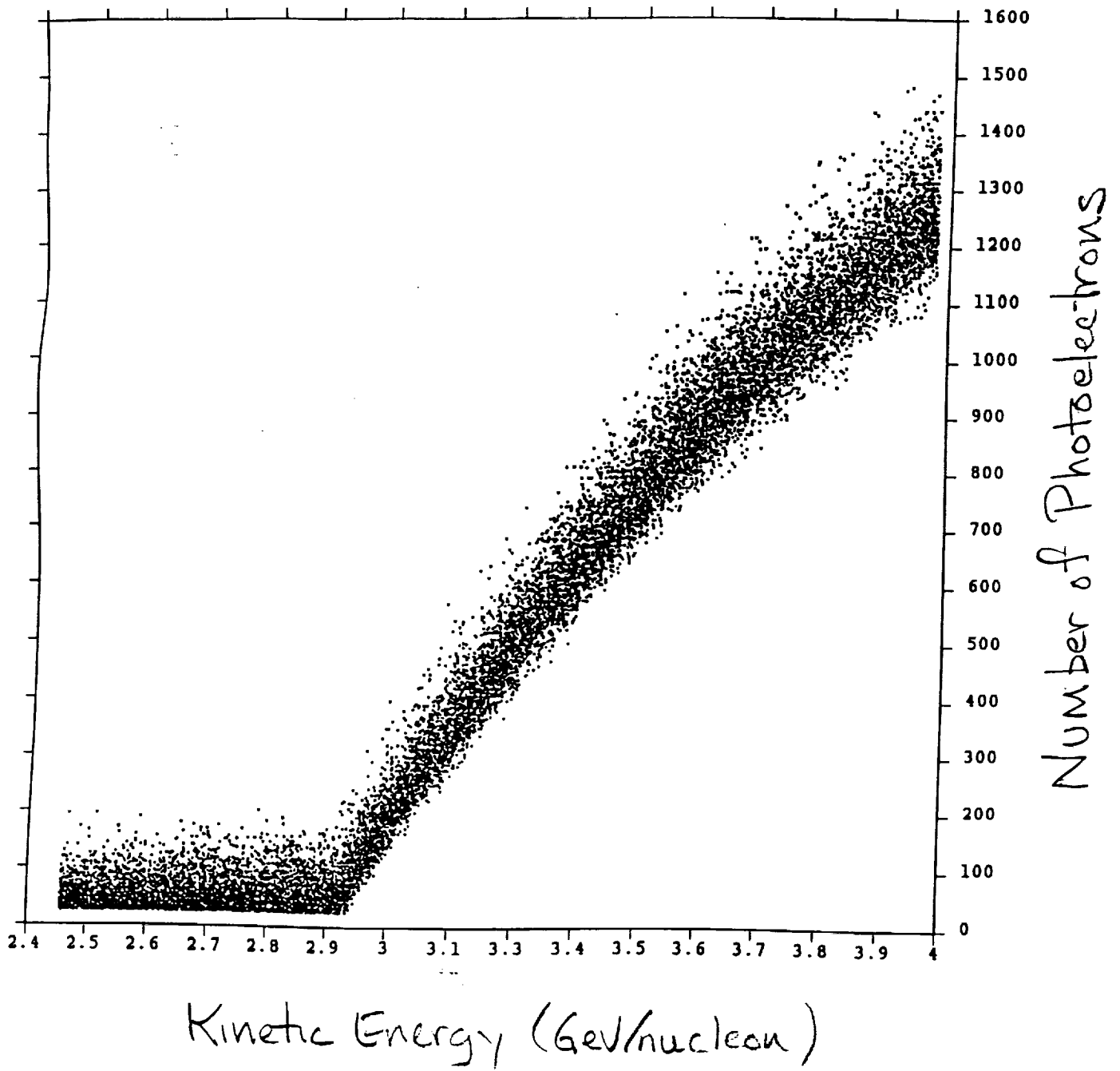


Figure 5

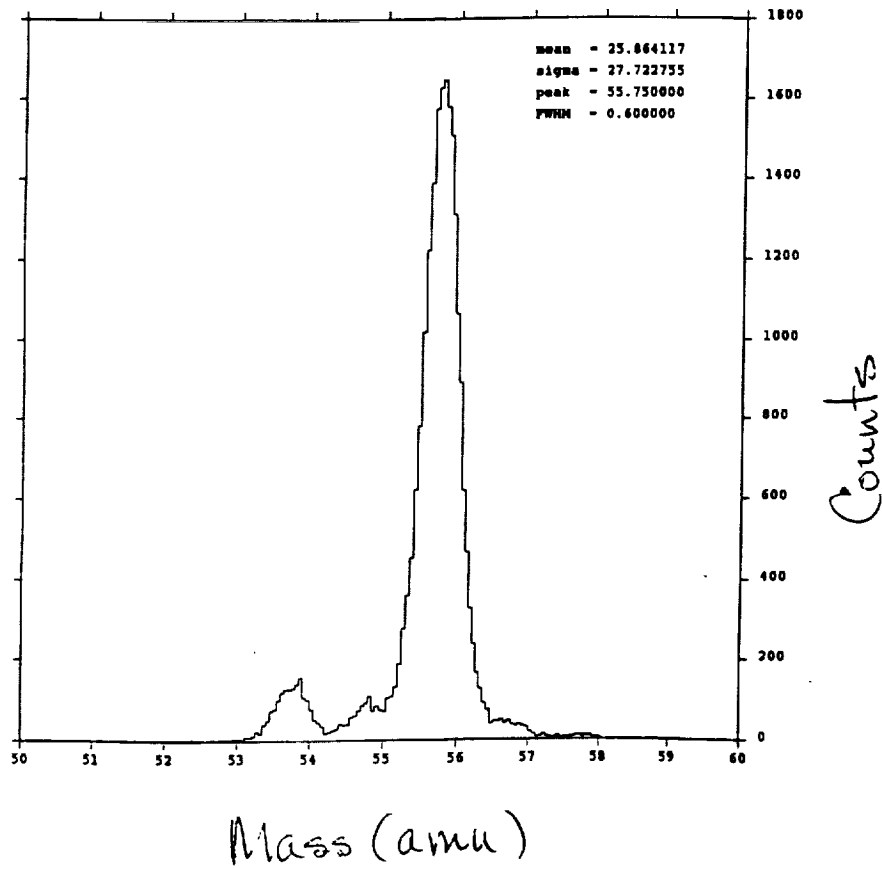
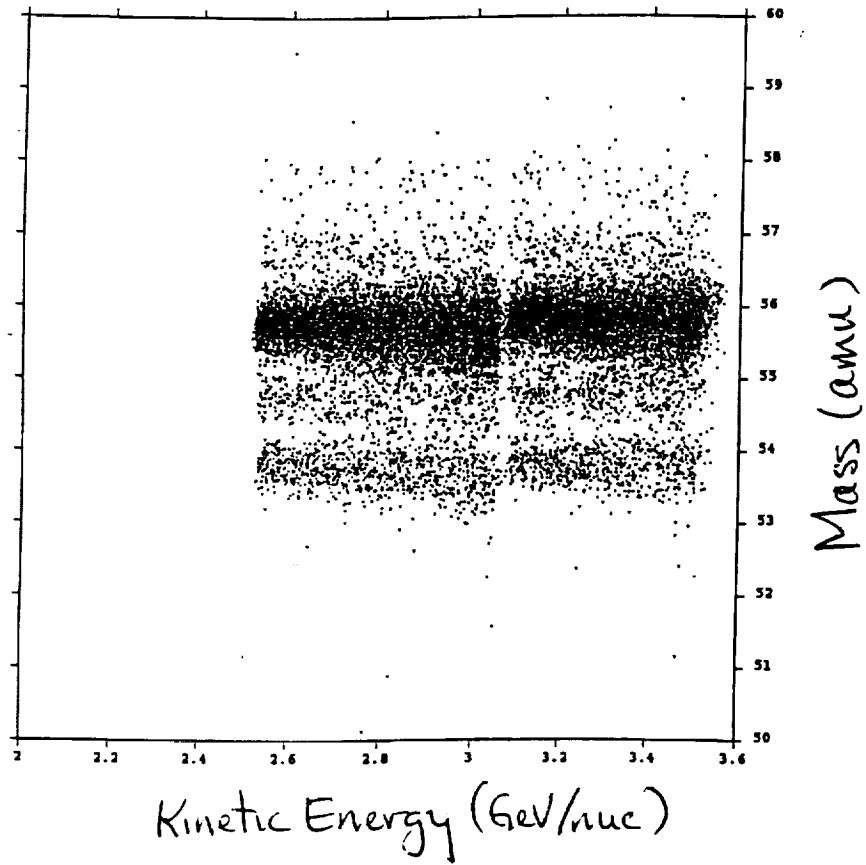


Figure 6

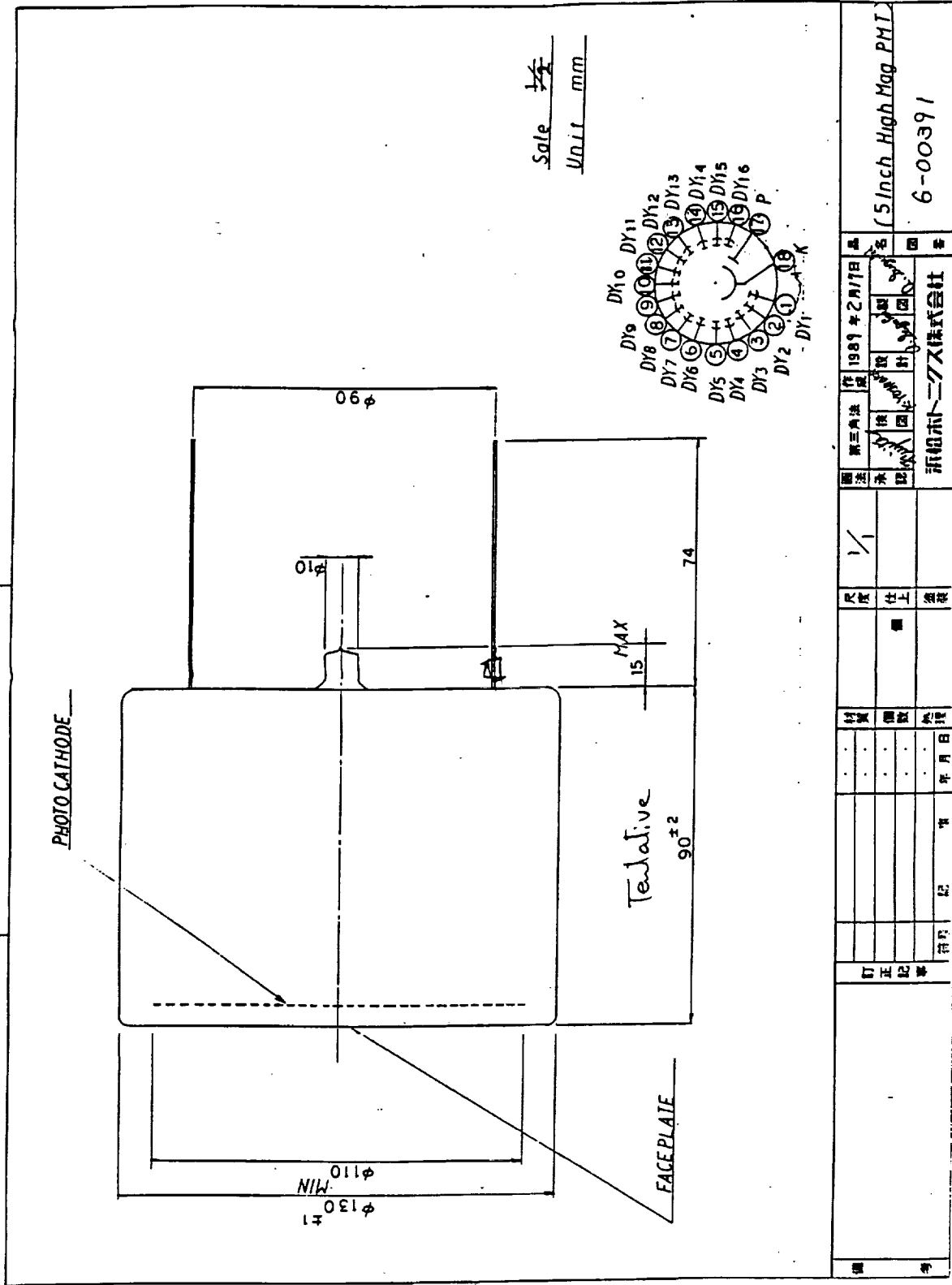


Figure 7

Tentative schematic of the new 5" tube being developed by Hamamatsu that will be tested under this grant. The tube is designed to operate in magnetic fields of many kiloGauss.

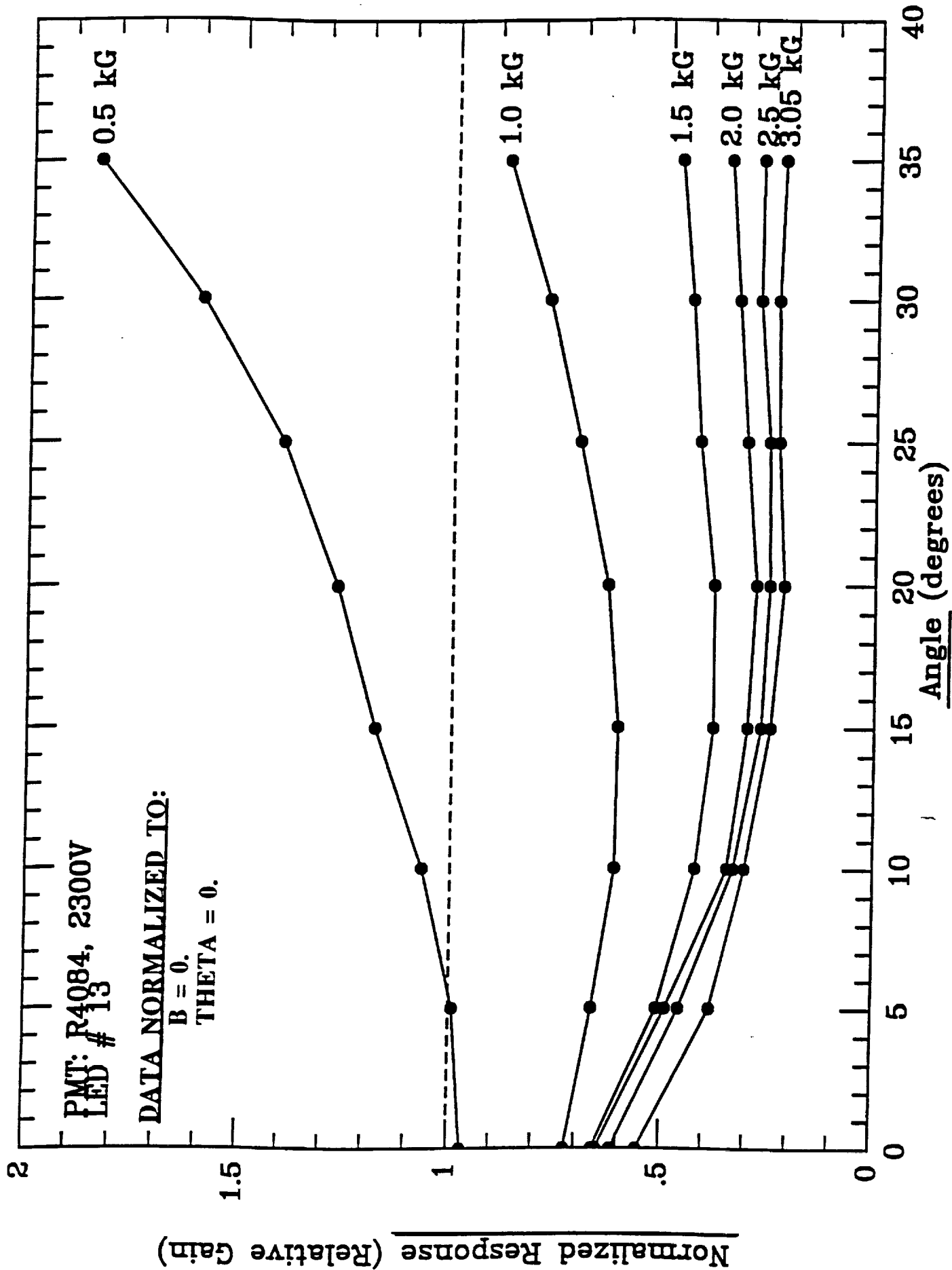


Figure 8

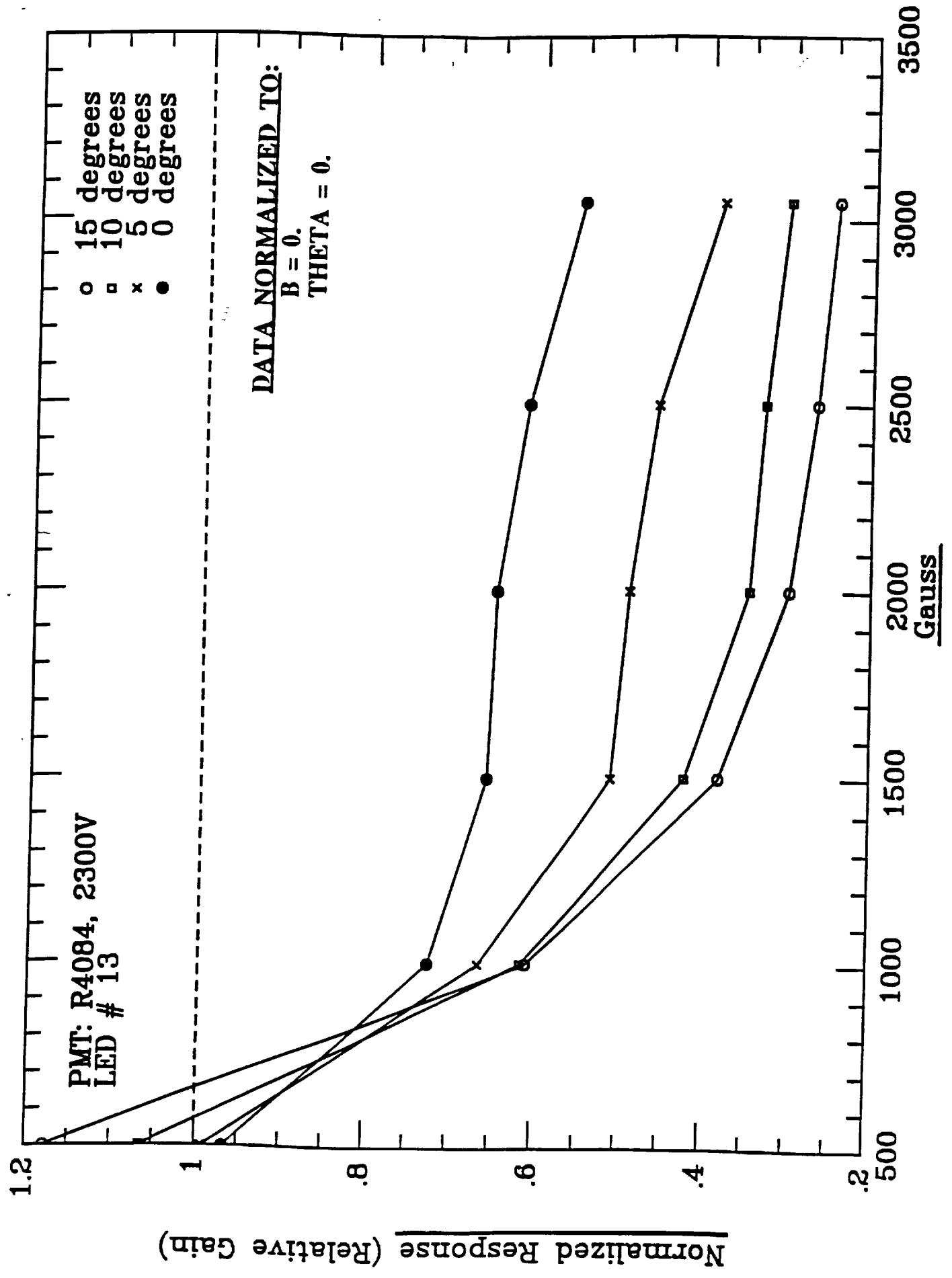


Figure 9

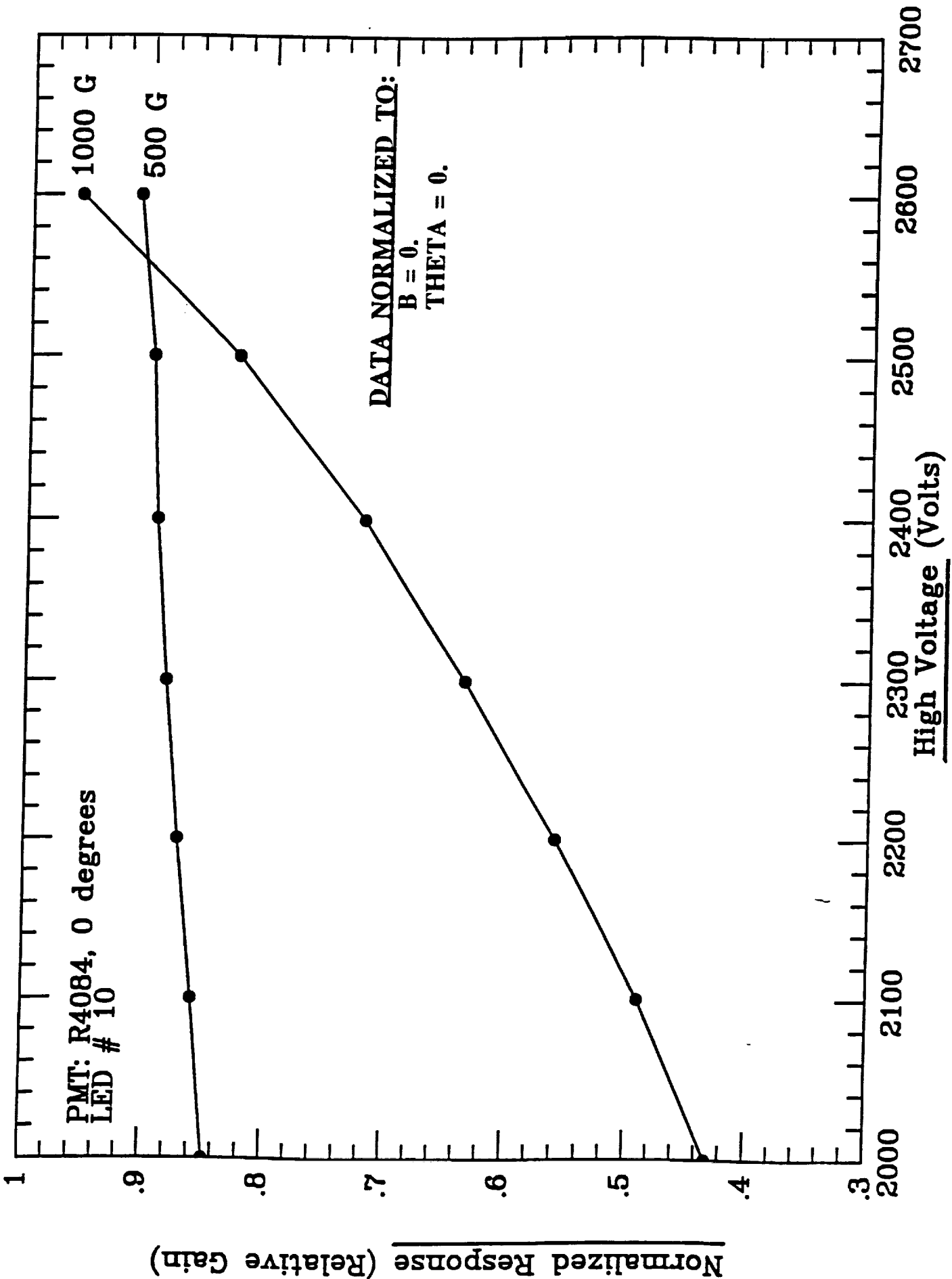


Figure 10

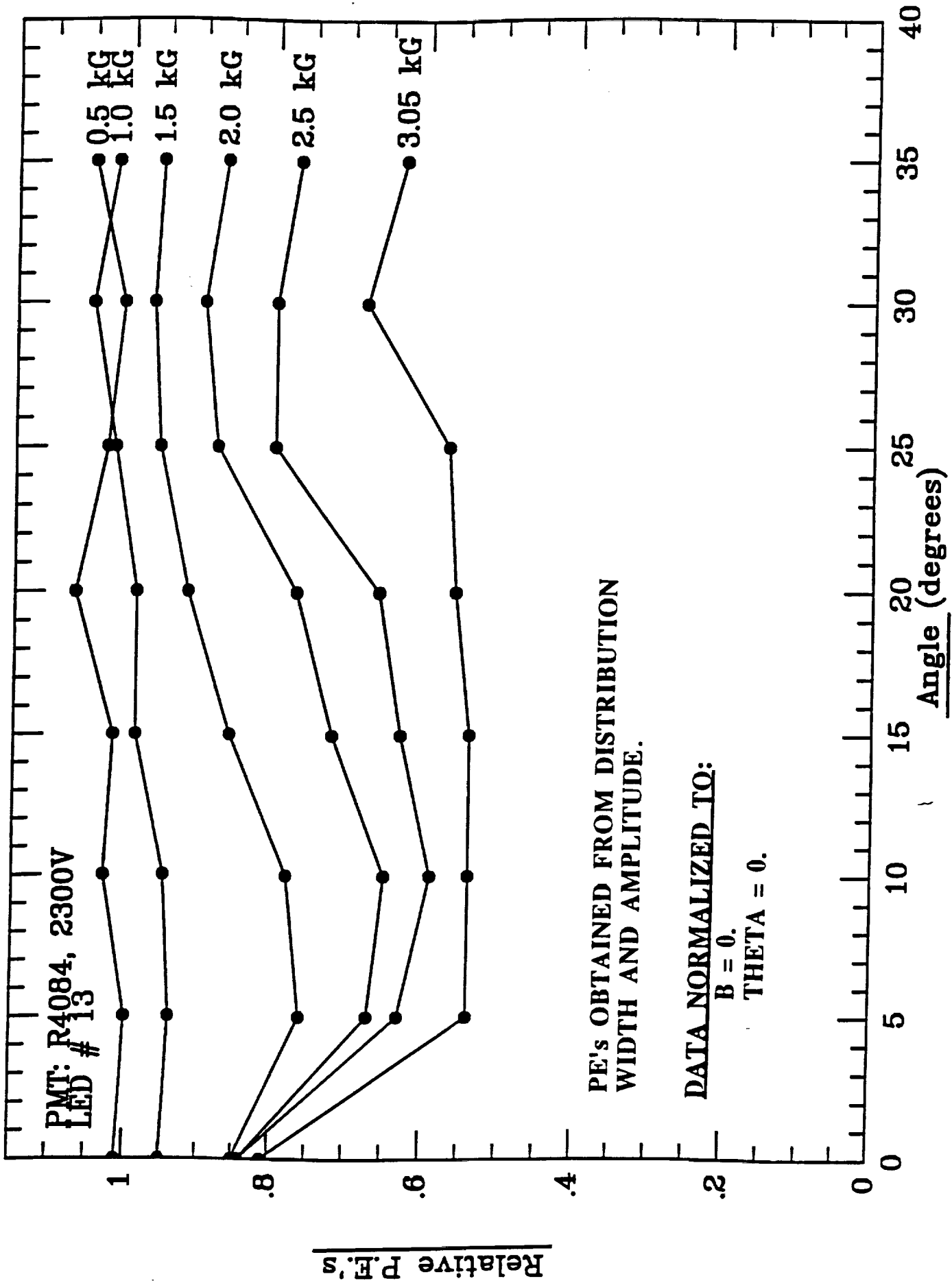
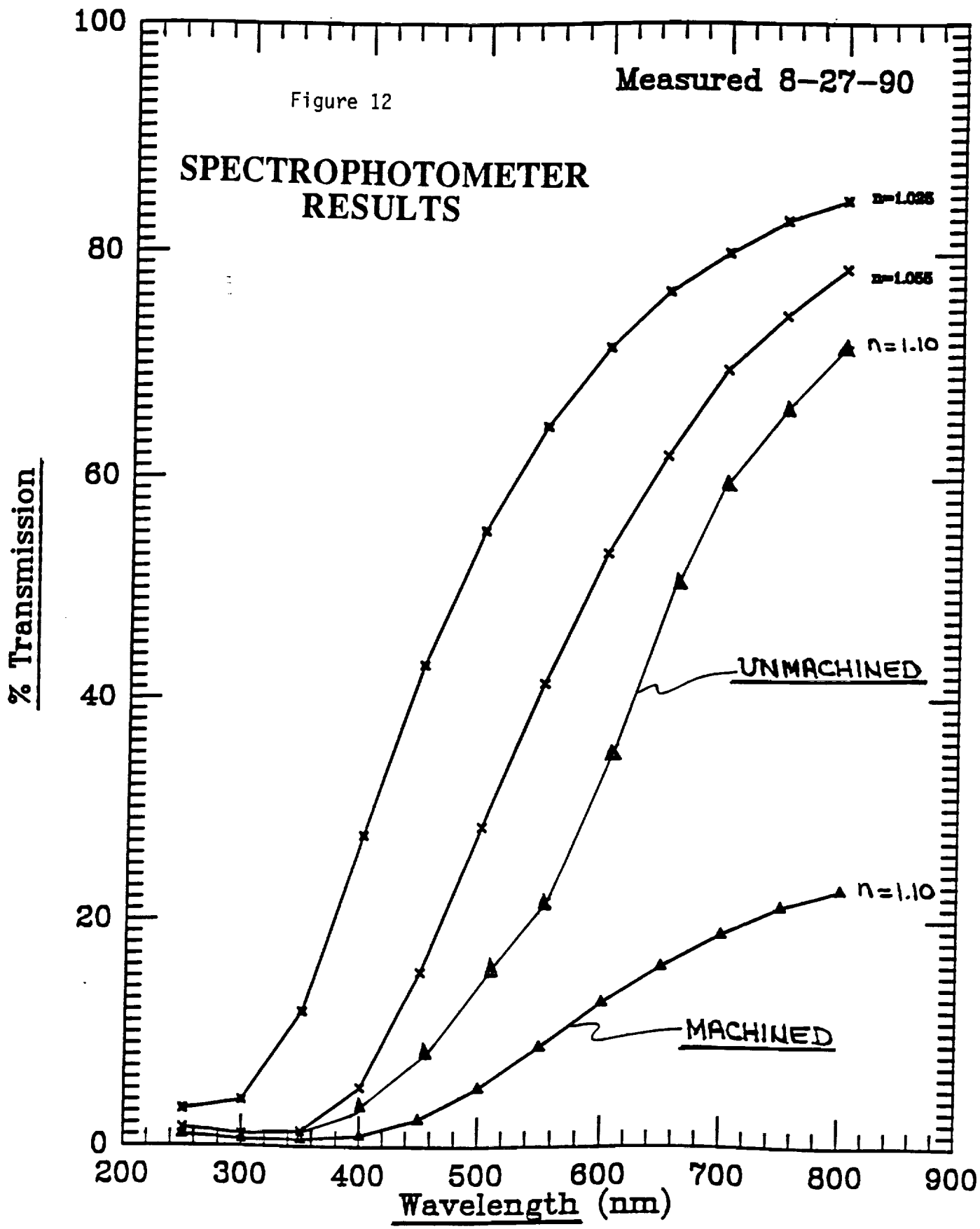


Figure 11

Measured 8-27-90

Figure 12

### SPECTROPHOTOMETER RESULTS



Aerogel block 4.75" x 4.75"  
Aerogel block 4.75" x 4.75" n=1.055  
Aerogel block 4.75" x 4.75" n=1.025

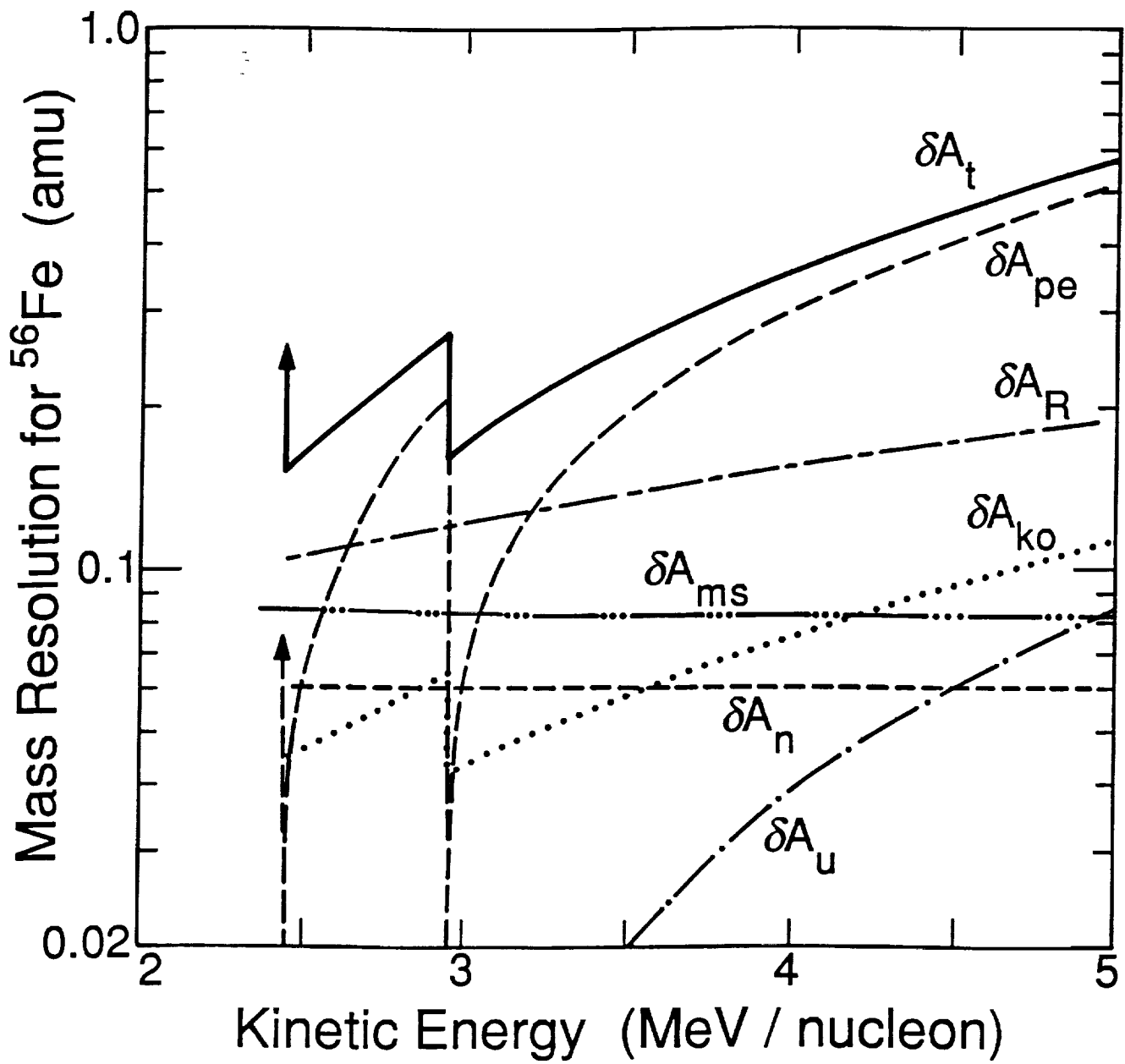


Figure 13